Liquid Crystals
Publication details, including instructions for authors and subscription information:
http://www.informaworld.com/smpp/title~content=t713926090

Director field of birefringent stripes in liquid crystal/nanoparticle dispersions

Martin Urbanski[a]; Brandy Kinkead[ab]; Torsten Hegmann[b]; Heinz-S. Kitzerow[a]
[a] Department of Chemistry, Faculty of Science, University of Paderborn, Paderborn, Germany [b] Department of Chemistry, University of Manitoba, Winnipeg, Canada

Online publication date: 09 September 2010

To cite this Article Urbanski, Martin , Kinkead, Brandy , Hegmann, Torsten and Kitzerow, Heinz-S.(2010) 'Director field of birefringent stripes in liquid crystal/nanoparticle dispersions', Liquid Crystals, 37: 9, 1151 — 1156
To link to this Article: DOI: 10.1080/02678292.2010.489160
URL: http://dx.doi.org/10.1080/02678292.2010.489160

Liquid Crystals,
Vol. 37, No. 9, September 2010, 1151–1156

Taylor & Francis
Taylor & Francis Group

Director field of birefringent stripes in liquid crystal/nanoparticle dispersions

Martin Urbanski[a], Brandy Kinkead[a,b], Torsten Hegmann[b] and Heinz-S. Kitzerow[a]*

[a]*Department of Chemistry, Faculty of Science, University of Paderborn, Paderborn, Germany;* [b]*Department of Chemistry, University of Manitoba, Winnipeg, Canada*

(*Received 2 March 2010; final version received 23 April 2010*)

The thermal stability, alignment and electro-optic properties of liquid crystals can be fundamentally altered by dispersing small amounts of solid nanoparticles in a liquid crystal host. In the present study, the local alignment of the liquid crystal in such dispersions is studied by means of polarising optical microscopy and fluorescence confocal polarising microscopy. The results of two- and three-dimensional imaging indicate that birefringent stripes, which are induced by the presence of nanoparticles, correspond to twist disclinations that are located at the liquid crystal–substrate interface. The luminescence of dispersed semiconductor quantum dots shows that the ends of disclination threads are pinned to conglomerates of nanoparticles, which stabilise these line defects.

Keywords: liquid crystals; nanocrystals; disclinations; fluorescence confocal polarising microscopy

1. Introduction

The dispersion of solid nanoparticles in liquid crystals offers unique opportunities to alter the properties of these anisotropic fluids. Calamitic liquid crystals are ordered fluids consisting of rod-like molecules, which tend to align parallel to each other. This orientational order causes anisotropic properties such as (uniaxial) birefringence, dielectric anisotropy, etc. The local alignment direction, which can be described by a pseudo-vector (director), is very sensitive to the anchoring at interfaces, to elastic forces, and to electric or magnetic fields [1]. This sensitivity is used, for example, in flat panel displays. Colloidal particles and nanoparticles dispersed in a liquid crystal can change its properties significantly [2]. For example, the dispersion of ultra-small magnetic needles [3, 4] or platelets [5] in nematic liquid crystals leads to ferronematics [3–6], which can be reoriented by very weak magnetic fields. Ferronematics can also be biased by magnetic fields, which leads to threshold-less optical switching in an electric field [6]. Dispersion of silica aerogel nanoparticles leads to filled nematics [7], which can be used for a laser-addressed reversible display. Ferroelectric nanoparticles can enhance the dielectric anisotropy [8] and the orientational order [9] of nematic liquid crystals, while metallic nanoparticles can increase the conductivity by several orders of magnitude [10].

In addition to nanoparticles changing the liquid crystal properties, a liquid crystalline host can also influence the arrangement of anisotropic particles. For example, anchoring at particle surfaces and elastic forces of the liquid crystal can direct colloidal particles to form chains along certain directions [11, 12] or two-dimensional colloidal crystals [13]. Sheet-like clay nanoparticles tend to form stacks in a nematic solvent [14] and their alignment in external fields is governed by the liquid crystal [15]. Carbon nanotubes can be uniaxially aligned in a thermotropic [16] or lyotropic [17, 18] liquid crystal. In recent years, Hegmann and co-workers have reported several observations which indicate that the alignment [2, 19] and the electro-optic switching behaviour [2, 20] of nematic liquid crystals are changed when nanoparticles made of gold [19, 20] or inorganic semiconductors (for example, CdSe or CdTe) [21] are dispersed in the respective liquid crystal. In samples where the pure liquid crystals show an alignment perpendicular to the glass surfaces (homeotropic alignment), the presence of nanoparticles may cause the appearance of birefringent stripes, which indicate a deviation from the homeotropic alignment. In samples where the molecules of the pure liquid crystal align parallel to the glass substrate, respective nanoparticle dispersions may cause a homeotropic alignment and even an inverted electro-optic switching characteristic. So far, the precise mechanisms of these unusual effects are unknown. The present study aims to clarify the origin and director field topology of the birefringent stripes that were observed in homeotropic samples [19]. In addition to conventional polarising optical microscopy (POM), the method of fluorescence confocal polarising microscopy (FCPM) was applied. The latter method allows three-dimensional imaging of the local director orientation by measuring the fluorescence intensity of a dichroic dye dissolved in the liquid crystal [22].

*Corresponding author. Email: Heinz.Kitzerow@upb.de

ISSN 0267-8292 print/ISSN 1366-5855 online

DOI: 10.1080/02678292.2010.489160
http://www.informaworld.com

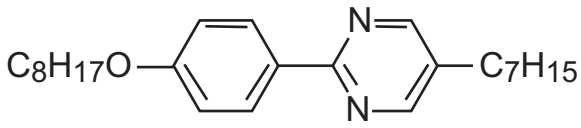

Scheme 1.

2. Experimental details

In the present study, the liquid crystal 5-n-heptyl-2-(4-n-octyloxy-phenyl)-pyrimidin (FELIX-2900-03, Clariant) was utilised as a host material. This compound, on heating, shows the phase sequence Crystalline, 52°C – [Smectic A, 45°C] – Nematic, 70°C – Isotropic liquid.

Gold nanoparticles either capped with n-hexyl-mercaptane (diameter 1.6 nm) or n-dodecylmercaptane (5.4 nm) were synthesised using the method by Brust and Schiffrin [20, 23]. Samples doped with 1 wt% of these nanoparticles show the typical formation of birefringent stripes observed by Hegmann *et al.* [2, 19, 20] at the phase transition from the isotropic to the nematic phase. For FCPM studies, the dichroic dye N,N'-bis(2,5-di-tert-butylphenyl)-3,4,9,10-perylendicarboximide (BTBP, 0.001–0.01%) was added to the liquid crystal/nanoparticle dispersion. This dye shows a bright fluorescence at $\lambda = 540$ nm and a high dichroic ratio. The spatial distribution of the nanoparticles was studied by using luminescent CdSe quantum dots instead of gold nanoparticles. For this purpose, CdSe particles capped with hexadecylamine (Sigma Aldrich) with a diameter of about 4.9 nm were used [21]. These particles show photoluminescence at a wavelength of $\lambda = 610$ nm, which can be separated from the organic dye luminescence using a spectrograph.

FCPM measurements were made using an Alpha300 confocal microscope (WiTec, Germany) equipped with an argon ion laser (488 nm) for excitation and a SpectraPro-2300i spectrograph (Princeton Instruments / Acton, $f = 300$ mm, *f*/3.9 imaging, grating: 600 lines/mm^{-1}) with a Peltier-cooled Andor CCD detector (model DV-401-BV). In addition to the standard equipment, the microscope was equipped with a polariser, a quarter wave-plate, and an analyser for polarisation control. The beam splitter cube was replaced by an interference beam splitter, which preserves the state of polarisation. These modifications enable the illumination of the sample with linearly polarised (lp) and circularly polarised (cp) light. In order to study both the polar and the azimuthal orientation of the molecules, the state of polarisation needs to be modified. If the transition dipole moment is aligned along the director $\mathbf{n} = (\sin\vartheta\cos\varphi, \sin\vartheta\sin\varphi, \cos\vartheta)^{\mathrm{T}}$, the light propagates along the z-direction and is linearly (for example, x-) polarised, and if only the linearly x-polarised component of the light emitted from the dichroic dye is detected, the local fluorescence intensity is approximately given by

$$I_{\mathrm{lp}} = I_{\max}\cos^4\alpha = I_{\max}\cos^4\varphi\sin^4\vartheta,$$

where α is the angle between the electric field of the light and the transition dipole moment of the dye [22]. In contrast to I_{lp}, the fluorescence intensity I_{cp} originating from circularly polarised excitation (and detected without any analyser) depends only on the polar alignment angle ϑ:

$$I_{\mathrm{cp}} = \tfrac{1}{2}\, I_{\max}\sin^2\vartheta.$$

Thus, the local director orientations can be probed by measuring both I_{lp} and I_{cp}.

3. Results

The prepared cells were heated up to the isotropic phase and then slowly (2°C min^{-1}) cooled down. Measurements were performed at 3°C below the phase transition into the nematic phase. Under these conditions, the image of the samples under POM shows dark areas and bright stripes (Figure 1). Under rotation of the sample between crossed polarisers, the dark areas remain dark. This seemingly isotropic behaviour indicates a director alignment perpendicular to the substrates (homeotropic alignment). In contrast, the intensity profile of the bright stripes changes, depending on the angle γ between the stripe axis and the plane of polarisation of the incident light. The stripes are dark if the angle γ is 0° or 90°, and exhibit a varying, but always symmetric, intensity profile for $0° < \gamma < 90°$, with maximum brightness at $|\gamma| = 45°$ (Figure 1). This typical birefringent behaviour indicates a planar, or at least partially planar, director alignment in the centre of the stripes. Different kinds of director field deformations can cause this transition of the director from perpendicular to planar alignment (Figure 2). The director may bend (Figure 2(a)), twist (Figure 2(c)) or show a combination of splay, twist and bend (Figure 2(b)). The latter possibility can be excluded by POM, since the corresponding director field (Figure 2(b)) should result in non-symmetrical intensity distributions. In addition, the complete extinction of the transmitted light along the transverse direction observed for $\gamma = 0°$ and $\gamma = 90°$ (Figure 1) indicates that either the director component along the stripe axis (Figure 2(a)) or the director component perpendicular to the stripe axis (Figure 2(c)) remains zero while the director changes gradually from homeotropic to planar alignment.

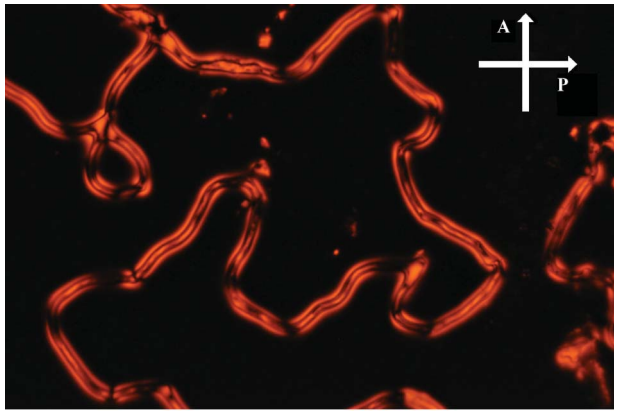

Figure 1. Image of a liquid crystal dispersion consisting of 3% (by weight) gold nanoparticles (diameter 5.4 nm) capped with dodecylthiol dispersed in Felix-2900-03. The image was obtained by polarising optical microscopy using monochromatic light ($\lambda = 589$ nm) and crossed polarisers. The planes of polarisation of polariser and analyser correspond to the horizontal and vertical direction in this image, respectively.

In order to distinguish between the director fields represented in Figure 2(a) and Figure 2(c), FCPM measurements were performed. The FCPM image obtained with circular polarised light shows two bright birefringent stripes on a dark background (Figure 3(a)). This confirms the homeotropic alignment of the liquid crystal in the uniform-appearing areas of the cell, while the orientation of the director within the stripes is rather planar. The bright spots are caused by agglomerations of undissolved fluorescence dye. Further information about the orientation of the director within the birefringent stripes was obtained by two measurements with linearly polarised light (Figure 3(b) and (c)). While the measurement with polarised light parallel to the *y*-axis (Figure 3(b)) shows only the vertical parts of the stripes, the measurement with polarised light parallel to the *x*-axis of the microscope (Figure 3(c)) shows only the horizontal parts of the birefringent stripes. This strongly indicates that the molecules in the defect line are aligned parallel to the defect line. Hence, this defect line corresponds to a twist disclination (Figure 2(c)).

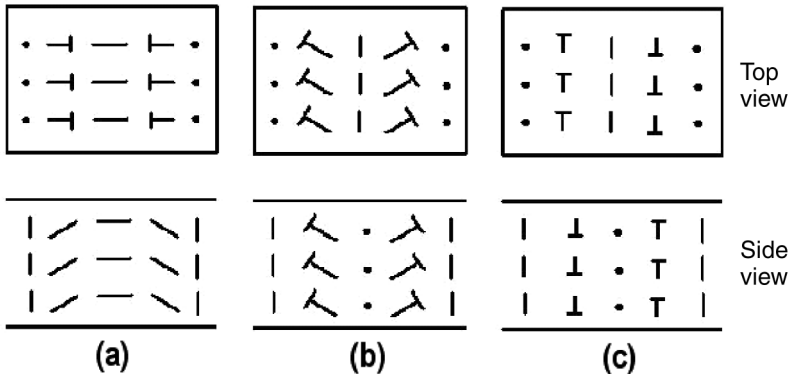

Figure 2. Possible director configurations that can lead to birefringent stripes appearing in a homeotropically aligned (and thus seemingly isotropic) surrounding. (a) Director field with bend deformation; (b) splay, twist and bend deformation; and (c) twist deformation, respectively.

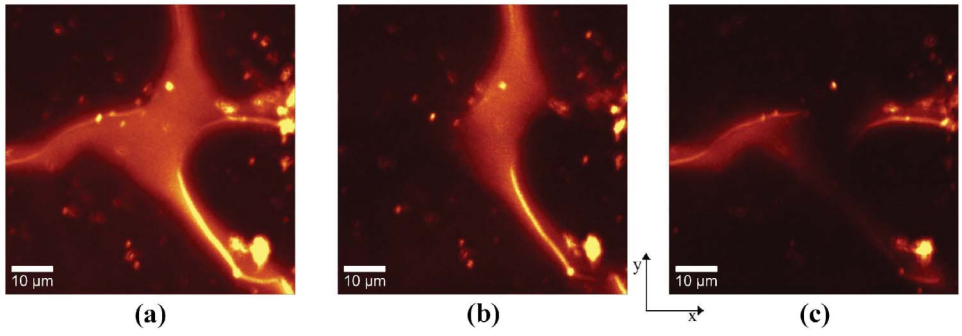

Figure 3. Fluorescence confocal polarising microscopy image of a sample obtained by adding 0.01% (by weight) of the dichroic fluorescent dye BTBP to the dispersion shown in Figure 1. Illumination with (a) circularly polarised light; (b) linearly polarised light (**E** vertical); and (c) linearly polarised light (**E** horizontal), respectively.

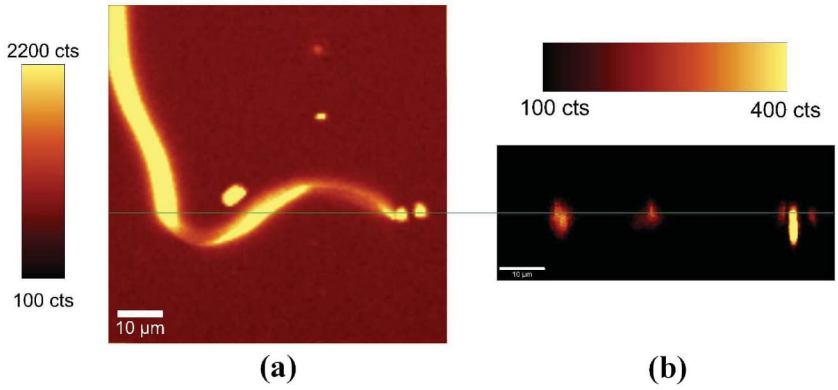

Figure 4. (a) Fluorescence confocal polarising microscopy (FCPM) top view [(x,y) plane] and (b) FCPM side view [(x,z) plane] of a gold nanoparticle dispersion. Composition of the sample: 3% (by weight) gold particles capped with hexylthiol and 0.01% (by weight) of the dichroic fluorescent dye BTBP in the nematic liquid crystal Felix-2900-03 (colour version online).

By performing (x,z) scans, the depths of the birefringent regions was investigated in a sample doped with 3% (by weight) of gold nanoparticles capped with hexylthiol. The bright spot on the right side of the image in Figure 4(b) shows an agglomeration of undissolved dye. Its size along the z-direction corresponds approximately to the thickness of the cell. However, the two signals to the left in Figure 4(b) are caused by the birefringent stripe. Their deepness is obviously smaller than the cell gap. Although the location of the glass plates can not be seen due to the homeotropic alignment of the liquid crystal, it is striking that all signals end at the same altitude in the (x,z) scan. This is a strong hint that the upper glass plate is located at this height. In conclusion, the experiment indicates that the birefringent stripes do not fill the gap completely, but seem to be fixed at one glass substrate of the cell.

After the phase transition and the formation of the birefringent stripe patterns, many stripes disappear in some samples after a few minutes, especially those that do not form closed loops. Open-ended stripes are usually unstable and mostly disappear during the measurement. However, it is interesting to note that a very few open-ended stripes seem to be even more stable than some closed loops. In order to study them in more detail, we investigated the stabilisation process of these open-ended birefringent stripes in a sample of FELIX-2900-03 doped with 0.001% (by weight) of the dichroic dye BTBP and 1% (by weight) of CdSe nanoparticles. Since these nanoparticles show a maximum fluorescence emission at 610 nm, the signals from dye (540 nm) and from CdSe (610 nm) could be separated using a spectrometer. The resulting FCPM images (Figure 5) show that the open-ended stripes are stabilised by agglomerations of nanoparticles. An FCPM image showing the total fluorescence intensity (not analysed by a spectrometer) shows both the bright disclination lines and bright spots at their ends (Figure 5(a)). However, the fluorescence image taken at the wavelength of $\lambda = 540$ nm (corresponding to the luminescence from the dichroic dye only) shows dark spots at the ends of the disclination lines, indicating a lack of dye at these positions. In contrast, the FCPM image taken at $\lambda = 610$ nm (corresponding to luminescence from the CdSe nanoparticles) shows bright spots at the ends of the disclination lines, indicating an agglomeration of CdSe particles at these positions (Figure 5(c)). It can be concluded that the ends of open disclination lines are pinned to nanoparticle agglomerations and thereby stabilised. Far away from these agglomerations, the nanoparticle fluorescence along the cross-section of the disclination lines is rather uniform.

The measurements do not confirm an enhancement of the particle concentration in the regions of twist deformation (as suggested by Qi and Hegmann's Figure 8(b) [19]). This experimental result is in agreement with considerations by other authors [24, 25]. Admittedly, phase fronts can drag [24] and defects can attract small particles [25] thereby enhancing the particle concentration at defect locations. However, this requires exceeding a critical particle radius, which was estimated to be $R_{\min} \approx 0.01$ µm [24] and $R_C \approx 0.2$ µm [25], respectively. Clearly, the size of isolated nanoparticles as studied here does not exceed this critical radius.

4. Conclusions

The presented FCPM studies show that the birefringent stripes observed in liquid crystalline nanoparticle dispersions earlier [2, 19, 20] correspond to twist disclinations. From the (x,z) scan, it can be concluded that the defects are not walls, which extend through the entire cell gap, but lines that are located at the substrate surface. In addition to closed-loop disclination lines, open-ended line defects also appear. The latter are stabilised by agglomerations of nanoparticles, and their presence

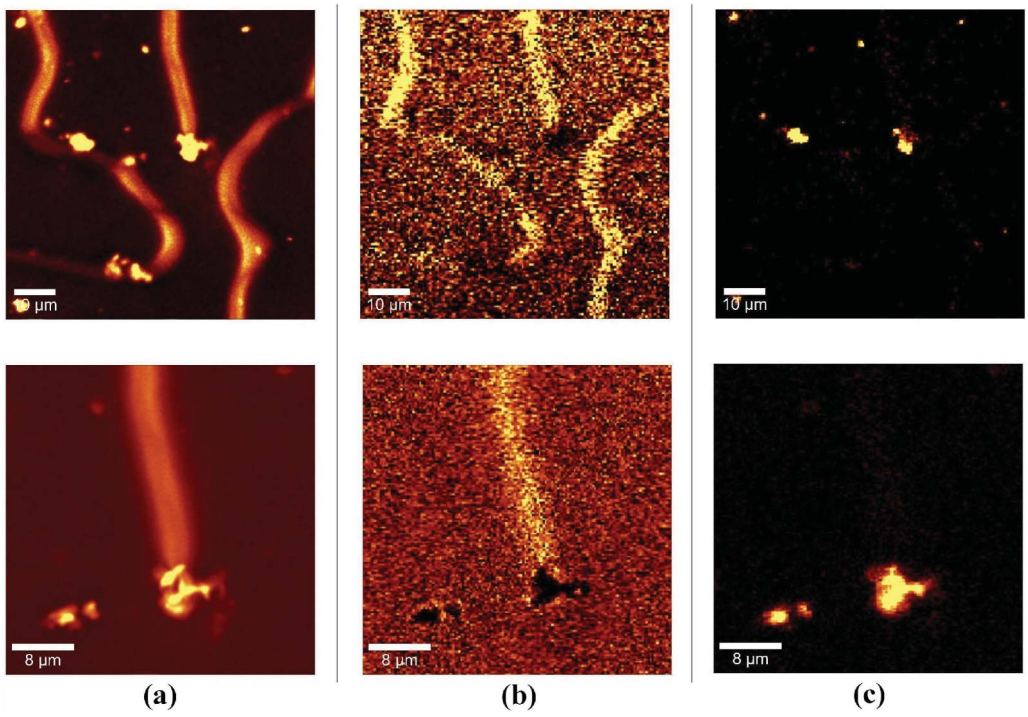

Figure 5. Fluorescence confocal polarising microscopy image of a sample consisting of 1% (by weight) CdSe nanoparticles, 0.001% (by weight) of the dichroic fluorescent dye BTBP, and the nematic liquid crystal Felix-2900-03. (a) Total fluorescence intensity (measured by an avalanche photodiode without spectrograph); (b) fluorescence intensity originating from the dichroic dye BTBP only ($\lambda = 540$ nm); and (c) fluorescence intensity originating from CdSe nanoparticles only ($\lambda = 610$ nm) (colour version online).

in these locations explains the unusual stability of these line defects, which is not observed in nanoparticle-free liquid crystals. In conclusion, the results of the present work allowed us to understand the intriguing defect formation in these nanoparticle-doped nematic liquid crystals, and will pave the way for designing defect-free nanoparticle/liquid crystal dispersions with great promise for applications in electro-optic devices operating, for example, at lower operating voltages [20, 21].

Acknowledgements

The authors would like to thank Alexander Lorenz for his kind assistance with photography (Figure 1). Financial support by the Deutsche Forschungsgemeinschaft (DFG, KI 411), the European Science Foundation (ESF-EUROCORES, SONS II program, LCNANOP project), the Natural Sciences and Engineering Research Council of Canada (NSERC), and the Technology Transfer Office (TTO) of the University of Manitoba for an IPM grant is gratefully acknowledged. BK would like to thank NSERC for an USRA.

References

[1] De Gennes, P.G.; Prost, J. *The Physics of Liquid Crystals*, 2nd ed.; Clarendon Press: Oxford, 1993.
[2] Qi, H.; Hegmann, T. *J. Mater. Chem.* **2008**, *18*, 3288–3294.
[3] Brochard, F.; de Gennes, P.G. *J. Phys. France* **1970**, *31*, 691–708.
[4] Rault, J.; Cladis, P.E.; Burger, J.P. *Phys. Lett. A* **1970**, *32*, 199–200.
[5] Hayes, C.F. *Mol. Cryst. Liq. Cryst.* **1976**, *36*, 245–253.
[6] Liang, B.J.; Chen, S.-H. *Phys. Rev. A: At., Mol., Opt. Phys.* **1989**, *39*, 1441–1446.
[7] Kreuzer, M.; Tschudi, T.; de Jeu, W.H.; Eidenschink, R. *Appl. Phys. Lett.* **1993**, *62*, 1712–1714.
[8] Ouskova, E.; Buchnev, O.; Reshetnyak, V.; Reznikov, Y.; Kresse, H. *Liq. Cryst.* **2003**, *30*, 1235–1239.
[9] Li, F.; Buchnev, O.; Cheon, C.I.; Glushchenko, A.; Reshetnyak, V.; Reznikov, Y.; Sluckin, T.J.; West, J.L. *Phys. Rev. Lett.* **2006**, *97*, 147801.
[10] Holt, L.A.; Bushby, R.J.; Evans, S.D.; Burgess, A.; Seeley, G. *J. Appl. Phys.* **2008**, *103*, 063712.
[11] Cladis, P.; Kléman, M.; Pieranski, P. *C. R. Hebd. des Seances Acad. Sci., Ser. B* **1971**, *273*, 275.
[12] Poulin, P.; Stark, H.; Lubensky, T.C.; Weitz, D.A. *Science* **1997**, *275*, 1770–1773.
[13] Muševič, I.; Škarabot, M.; Tkalec, U.; Ravnik, M.; Žumer, S. *Science* **2006**, *313*, 954–958.
[14] Pizzey, C.; Klein, S.; Leach, E.; van Duijneveldt, J.S.; Richardson, R.M. *J. Phys.: Condens. Matter* **2004**, *16*, 2479–2495.
[15] Connolly, J.; van Duijneveldt, J.S.; Klein, S.; Pizzey, C.; Richardson, R.M. *J. Phys. Condens. Matter* **2007**, *19*, 156103.
[16] Dierking, I.; Scalia, G.; Morales, P.; LeClere, D. *Adv. Mater. (Weinheim, Ger.)* **2004**, *16*, 865–869.

[17] Lagerwall, J.; Scalia, G.; Haluska, M.; Dettlaff-Weglikowska, U.; Roth, S.; Giesselmann, F. *Adv. Mater. (Weinheim, Ger.)* **2007**, *19*, 359–364.
[18] Lagerwall, J.P.F.; Scalia, G. *J. Mater. Chem.* **2008**, *18*, 2890–2898.
[19] Qi, H.; Hegmann, T. *J. Mater. Chem.* **2006**, *16*, 4197–4205.
[20] Qi, H.; Kinkead, B.; Hegmann, T. *Adv. Funct. Mater.* **2008**, *18*, 212–221.
[21] Kinkead, B.; Hegmann, T. *J. Mater. Chem.* **2010**, *20*, 448–458.
[22] Smalyukh, I.I.; Shiyanovskii, S.V.; Lavrentovich, O.D. *Chem. Phys. Lett.* **2001**, *336*, 88–96.
[23] Brust, M.; Walker, M.; Bethell, D.; Schiffrin, D.J.; Whyman, R. *Chem. Commun.* **1994**, 801–802.
[24] West, J.L.; Glushchenko, A.; Liao, G.; Reznikov, Y.; Andrienko, D.; Allen, M.P. *Phys. Rev. E: Stat., Nonlinear, Soft Matter Phys.* **2002**, *66*, 012702.
[25] Voloschenko, D.; Pishnyak, O.P.; Shiyanovskii, S.V.; Lavrentovich, O.D. *Phys. Rev. E: Stat., Nonlinear, Soft Matter Phys.* **2002**, *65*, 060701.